

1 **Resurrecting essential amino acid biosynthesis in a mammalian cell**

2

3 Julie Trolle^{1†}, Ross M. McBee^{2,3†}, Andrew Kaufman³, Sudarshan Pinglay¹, Henri Berger^{1‡},
4 Sergei German¹, Liyuan Liu³, Michael J. Shen^{1,4}, Xinyi Guo⁵, J. Andrew Martin^{1§}, Michael
5 Pacold⁶, Drew R. Jones⁷, Jef D. Boeke^{1,8*}, Harris H. Wang^{3*}

6

7 **Affiliations:**

8 ¹ Institute for Systems Genetics, Department of Biochemistry and Molecular Pharmacology,
9 NYU Langone Health; New York, NY, USA.

10 ² Department of Biological Sciences, Columbia University; New York, NY, USA.

11 ³ Department of Systems Biology, Columbia University; New York, NY, USA.

12 ⁴ Department of Internal Medicine, NYU Langone Health; New York, NY, USA.

13 ⁵ Department of Biology, New York University; New York, NY, USA.

14 ⁶ Department of Radiation Oncology, NYU Langone Health; New York, NY, USA.

15 ⁷ Department of Biochemistry and Molecular Pharmacology, NYU Langone Health; New York,
16 NY, USA.

17 ⁸ Department of Biomedical Engineering, NYU Tandon School of Engineering; Brooklyn, NY
18 11201, USA.

19

20 † These authors contributed equally to this work

21 * Correspondences should be addressed to hw2429@columbia.edu or

22 jef.boeke@nyulangone.org

23 ‡ Current address: Weill Cornell Graduate School of Medical Sciences; New York, NY, USA.

24 § Current address: Reopen Diagnostics, LLC; Queens, NY, USA.

25 MAIN TEXT

26

27 **Major genomic deletions in independent eukaryotic lineages have led to repeated ancestral**
28 **loss of biosynthesis pathways for nine of the twenty canonical amino acids¹. While the**
29 **evolutionary forces driving these polyphyletic deletion events are not well understood, the**
30 **consequence is that extant metazoans are unable to produce nine essential amino acids**
31 **(EAAs). Previous studies have highlighted that EAA biosynthesis tends to be more**
32 **energetically costly^{2,3}, raising the possibility that these pathways were lost from organisms**
33 **with access to abundant EAAs in the environment^{4,5}. It is unclear whether present-day**
34 **metazoans can reaccept these pathways to resurrect biosynthetic capabilities that were**
35 **lost long ago or whether evolution has rendered EAA pathways incompatible with**
36 **metazoan metabolism. Here, we report progress on a large-scale synthetic genomics effort**
37 **to reestablish EAA biosynthetic functionality in a mammalian cell. We designed codon-**
38 **optimized biosynthesis pathways based on genes mined from *Escherichia coli*. These**
39 **pathways were *de novo* synthesized in 3 kilobase chunks, assembled *in yeast* and**
40 **genomically integrated into a Chinese Hamster Ovary (CHO) cell line. One synthetic**
41 **pathway produced valine at a sufficient level for cell viability and proliferation, and thus**
42 **represents a successful example of metazoan EAA biosynthesis restoration. This**
43 **prototrophic CHO line grows in valine-free medium, and metabolomics using labeled**
44 **precursors verified *de novo* biosynthesis of valine. RNA-seq profiling of the valine**
45 **prototrophic CHO line showed that the synthetic pathway minimally disrupted the cellular**
46 **transcriptome. Furthermore, valine prototrophic cells exhibited transcriptional signatures**
47 **associated with rescue from nutritional starvation. This work demonstrates that**
48 **mammalian metabolism is amenable to restoration of ancient core pathways, thus paving**
49 **a path for genome-scale efforts to synthetically restore metabolic functions to the**
50 **metazoan lineage.**

51 Whole genome sequencing across the tree of life has revealed the surprising observation
52 that nine amino acid (AA) biosynthesis pathways are missing from the metazoan lineage¹.
53 Furthermore, these losses appear to have occurred multiple times during eukaryotic evolution,
54 including in some microbial lineages (**Fig 1A**)^{1,4}. Branching from core metabolism, the nine EAA
55 biosynthesis pathways missing from metazoans involve over forty genes (**Fig 1B, Table ED1-**
56 **ED3**), widely found in bacteria, fungi and plants⁴. While the absence of essential metabolic
57 pathways is observed in certain bacteria⁶, which possess short generation times and high
58 genomic flexibility to adapt to rapidly changing environments, the forces driving the loss of multiple

59 EAA biosynthetic pathways in multicellular eukaryotes remain a great mystery. Their partial
60 reacquisition through horizontal gene transfer in certain rare insect lineages with extremely simple
61 nutrient sources, such as sap or blood, enables them to host genome-reduced intracellular
62 bacteria that provide other missing metabolites missing from these limited diets, and provides the
63 “exception that proves the rule”⁷. Recent efforts in genome-scale synthesis⁸⁻¹⁰ and genome-
64 writing¹¹ have highlighted our increasing capacity to construct synthetic genomes with novel
65 properties, thus providing a route to not only examine these interesting evolutionary questions but
66 also yield new capacities of bioindustrial utility¹²⁻¹⁴.

67 We sought to explore the possibility of generating prototrophic mammalian cells capable
68 of complete biosynthesis of EAAs using a synthetic genomics approach (**Fig 1C**). The Chinese
69 Hamster Ovary (CHO) K1 cell line was chosen as a model system due to its fast generation time,
70 amenability to genetic manipulations, availability of a whole genome sequence, and established
71 industrial relevance for producing biologics¹⁵. EAA biosynthesis genes from the best
72 characterized model organisms were considered during pathway design while optimizing for the
73 fewest number of enzymes needed for a given EAA pathway. To avoid using multiple promoters,
74 we introduced ribosome-skipping 2A sequences¹⁶ between biosynthetic genes to allow for protein
75 translation of separate enzymes from a single transcriptional unit. The EAA pathway and an
76 additional EGFP reporter were placed in a vector that could be integrated as a single copy into
77 the CHO genome at a designated landing pad using the FLP-In system¹⁷. The entire pathway was
78 synthesized *de novo* by commercial gene synthesis in 3 kilobase fragments and assembled in
79 *Saccharomyces cerevisiae* via homologous recombination of 80 basepair overlaps. Subsequent
80 antibiotic selection of cells transfected with the vector resulted in a stable cell line containing the
81 integrated EAA pathway. Finally, we performed a variety of phenotypic, metabolomic, and
82 transcriptomic characterizations on the modified cell line to verify activity of the EAA biosynthesis
83 pathway.

84 We first confirmed that the CHO cell line was auxotrophic for each of the 9 EAAs. As
85 expected, CHO-K1 did not grow in “dropout” F-12K medium lacking each of the 9 EAAs and
86 supplemented with dialyzed FBS (**Fig S1**). We noted that in this cell line, canonically non-essential
87 amino acids tyrosine and proline also exhibited EAA-like properties in dropout media. Insufficient
88 concentrations of phenylalanine in F-12K media or low expression of endogenous phenylalanine-
89 4-hydroxylase that converts phenylalanine to tyrosine could underlie tyrosine limitation. Proline
90 auxotrophy in CHO-K1 results from epigenetic silencing of the gene encoding Δ 1-pyrroline-5-
91 carboxylate synthetase (P5CS) in the proline pathway¹⁸. We therefore used proline as a test case
92 for our synthetic genomics pipeline. We tested the P5CS-equivalent proline biosynthesis enzyme

93 found in *E. coli*, encoded by two separate genes, *proA* and *proB* (**Fig ED2A**). A vector (pPro)
94 carrying codon-optimized *proA* and *proB* separated by a P2A sequence was synthesized and
95 integrated into CHO-K1 (**Fig ED2B**). CHO cells with the stably integrated pPro proline pathway
96 showed robust growth in proline-free medium (**Fig ED2C-D**), thus validating a pipeline for
97 designing and generating specific AA prototrophic cells.

98 To demonstrate restoration of EAA pathways lost from the metazoan lineage more than
99 650-850 million years ago¹⁹, we built a 6-gene construct (pMTIV) to test the simultaneous rescue
100 of methionine, threonine, isoleucine and valine auxotrophies. These EAAs were chosen because
101 their biosynthesis pathways were missing the fewest number of genes: methionine and threonine
102 production require two genes while valine and isoleucine require four genes total (**Fig ED3**). To
103 biosynthesize methionine, we chose the *E. coli metC* gene, which converts cystathionine to
104 homocysteine, a missing step in CHO-K1 cells in a potential serine to methionine biosynthetic
105 pathway. Threonine production was tested using *E. coli* glycine hydroxymethyltransferase *ItaE*,
106 which converts glycine and acetaldehyde into threonine. For branched chain amino acids
107 (BCAAs) valine and isoleucine, three additional biosynthetic enzymes and one regulatory subunit
108 are needed in theory to convert pyruvate and 2-oxobutanoate into valine and isoleucine,
109 respectively. In the case of valine, pyruvate is converted to 2-acetolactate, then to 2,3-dihydroxy-
110 isovalerate, then to 2-oxoisovalerate and finally to valine. For isoleucine, 2-oxobutanoate is
111 converted to 2-aceto-2-hydroxybutanoate, then to 2,3-dihydroxy-3-methylpentanoate, then to 3-
112 methyl-2-oxopentanoate, and finally to isoleucine. The final steps in both BCAAs can be
113 performed by native CHO catabolic enzymes Bcat1 and Bcat2¹⁸. In *E. coli*, the first three steps in
114 the pathway are embodied in four genes that encode an acetolactate synthase split into catalytic
115 and regulatory subunits (*ilvB/N*), a ketol-acid reductoisomerase (*ilvC*), and a dihydroxy-acid
116 dehydratase (*ilvD*) (**Fig 2A**)²⁰. The final pMTIV construct comprises *metC*, *itaE*, *ilvB*, *ilvN*, *ilvC* and
117 *ilvD*, organized as a single open reading frame (ORF) with a 2A sequence variant in between
118 each protein coding region (**Fig 2B**), driven by a strong SFFV viral promoter.

119 To test the biosynthetic capacity of pMTIV, we first introduced the construct into CHO
120 cells. Flp-In integration was used to stably insert either pMTIV, or a control vector (pCtrl) into the
121 CHO genome. Successful generation of each cell line was confirmed by PCR amplification of
122 junction regions formed during vector integration (**Fig ED4A-B**). RNA-seq of cells containing the
123 pMTIV construct confirmed transcription of the entire ORF (**Fig 2C**). Western blotting of pMTIV
124 cells using antibodies against the P2A peptide yielded bands at the expected masses of P2A-
125 tagged proteins, confirming the production of separate distinct enzymes (**Fig ED4C**).

126 In methionine-free, threonine-free, or isoleucine-free medium, cells containing the pMTIV
127 construct did not show viability over seven days, similar to cells containing the pCtrl control vector
128 **Fig ED5**). In striking contrast, however, cells containing the integrated pMTIV showed relatively
129 healthy cell morphology and viability in valine-free medium (**Fig 2D**), whereas cells containing
130 pCtrl exhibited substantial loss of viability over six days. In complete medium, cells carrying the
131 integrated pMTIV construct showed no growth defects compared to control cells (**Fig 2E**). In
132 valine-free medium, pMTIV cells showed a 32% increase in cell number over 6 days compared
133 to an 88% decrease in cell number in pCtrl cells (**Fig 2F**). When cultured in valine-free medium
134 over multiple passages with medium changes every two days, pMTIV cell proliferation was
135 substantially reduced by the 3rd passage. We hypothesized that frequent passaging might over-
136 dilute the medium and prevent sufficient accumulation of biosynthesized valine necessary for
137 continued proliferation. We thus deployed a “conditioned-medium” regimen whereby 50% of the
138 medium was freshly prepared valine-free medium and 50% was “conditioned” valine-free medium
139 in which pMTIV cells had previously been cultured over 2 days (see Methods). Using this regimen,
140 we were able to culture pMTIV cells for 9 passages without addition of exogenous valine, during
141 which time they exhibited an average doubling time of 8.5 days. However, the doubling time varied
142 across the 49 days of experimentation with cells exhibiting a mean doubling time of 5.3 days in
143 the first 24 days and 21.0 days in the last 25 days. The increase in doubling time seen in later
144 passages may be the result of detrimental effects from culturing cells longer-term in partially
145 recycled and dialyzed FBS or may result from variation in the cell number to medium volume ratio,
146 which trended downwards in later passaging events as cell growth slowed. Despite the slowed
147 growth seen in later passages, cells exhibited healthy morphology and continued to proliferate at
148 day 49, suggesting that the cells could have been passaged even further. To verify that the
149 putative valine rescue effect was due to the valine biosynthesis genes present in pMTIV
150 specifically, we constructed and tested a second EAA pathway vector pIV that only contained the
151 four genes *ilvNBCD*. The pIV construct similarly supported cell growth in valine-free medium, and
152 exhibited similar growth dynamics to the pMTIV construct in complete medium (**Fig ED5, Fig**
153 **ED6**).

154 To confirm endogenous biosynthesis of valine, we cultured pCtrl and pMTIV cells in RPMI
155 medium containing ¹³C₆-glucose in the place of its ¹²C equivalent together with ¹³C₃-pyruvate
156 spiked in at 2 mM over 3 passages (**Fig ED7A**). High-resolution MS1 of MTIV cell lysates revealed
157 a peak at 123.1032 *m/z*, the expected *m/z* for ¹³C₅-valine (**Fig 3A**). This detected peak was subject
158 to MS2 alongside a ¹²C-valine control peak and a ¹³C₅/¹⁵N-valine peak, which was spiked into all
159 samples to serve as an internal standard. The resulting fragmentation patterns for each peak (**Fig**

160 **3B**) matched the theoretical expectations for each isotopic version of valine (**Fig ED7B**). An
161 extracted ion chromatogram further revealed a peak in the pMTIV valine-free medium metabolite
162 extraction, which corresponded to a peak in the spiked-in positive control $^{13}\text{C}_5/^{15}\text{N}$ -valine, whereas
163 no equivalent peak was seen among metabolites extracted from pCtrl cells (**Fig ED7C**). Taken
164 together, this demonstrates that pMTIV cells are biosynthesizing valine from core metabolites
165 glucose and pyruvate, thereby representing successful metazoan biosynthesis of valine. Over the
166 course of 3 passages in heavy valine-free medium, the non-essential amino acid alanine, which
167 is absent from RPMI medium and synthesized from pyruvate, was found to be 86.1% ^{13}C -labeled
168 in pMTIV cell lysates. Assuming similar turnover rates for alanine and valine within the CHO
169 proteome, we expected to see similar percentages of ^{13}C -labeled valine. However, just 32.2% of
170 valine in pMTIV cell lysates was ^{13}C -labeled (**Fig ED7D-E**). For pMTIV cells cultured in heavy
171 complete medium, just 6.4% of valine in cell lysates was ^{13}C -labeled. Together with the observed
172 slow proliferation of pMTIV cells in valine-free medium, our data suggests that valine
173 complementation is sufficient but perhaps sub-optimal for cell growth.

174 We performed RNA-seq to profile the transcriptional responses of cells containing pMTIV
175 or pCtrl in complete (harvested at 0 h) and valine-free medium (harvested at 4 and 48 h,
176 respectively) (**Fig 3C, Fig ED8A**). The transcriptional impact of pathway integration is modest
177 (**Fig 3D**). Only 51 transcripts were differentially expressed between pCtrl and pMTIV cells grown
178 in complete medium, and the fold changes between conditions were small (**Fig 3E, Fig ED8B**).
179 While some gene ontology (GO) functional categories were enriched (**Fig ED8C**), they did not
180 suggest dramatic cellular stress. Rather, these transcriptional changes may reflect cellular
181 response to BCAA dysregulation due to alterations in valine concentrations²¹, or they may result
182 from cryptic effects of bacterial genes placed in a heterologous mammalian cellular context. In
183 contrast, comparison of 48 h valine-starved pCtrl and pMTIV cells yielded ~7,500 differentially
184 expressed genes. Transcriptomes of pMTIV cells in valine-free medium more closely resembled
185 cells grown on complete medium than did pCtrl cells in valine-free medium (**Fig 3D, Fig ED9A**).
186 Differentially expressed genes between pCtrl and pMTIV cells showed enrichment for hundreds
187 of GO categories, including clear signatures of cellular stress such as autophagy, changes to
188 endoplasmic reticulum trafficking, and ribosome regulation (**Fig ED9B**). Most of the differentially
189 regulated genes between pCtrl cells in complete medium, and those same cells starved of valine
190 for 48 hours were also differentially expressed when comparing pCtrl and pMTIV cells in valine-
191 free medium (**Fig 3E**), supporting the hypothesis that most of the observed transcriptional
192 changes represent broad but partial rescue of the cellular response to starvation.

193 In this work, we demonstrated the successful restoration of an EAA biosynthetic pathway
194 in a metazoan cell. Our results indicate that contemporary metazoan biochemistry can support
195 complete biosynthesis of valine, despite millions of years of evolution from its initial loss from the
196 ancestral lineage. Interestingly, independent evidence for BCAA biosynthesis has also been
197 obtained for sap-feeding whitefly bacteriocytes that host bacterial endosymbionts; metabolite
198 sharing between these cells is predicted to lead to biosynthesis of BCAAs that are limiting in their
199 restricted diet. The malleability of mammalian metabolism to accept heterologous core pathways
200 opens up the possibility of animals with designer metabolisms and enhanced capacities to thrive
201 under environmental stress and nutritional starvation²². Yet, our failure to functionalize designed
202 methionine, threonine and isoleucine pathways highlights outstanding challenges and future
203 directions. Other pathway components or alternative selections may be needed for different
204 EAAs²³. A general lack of predictability and a dearth of well-characterized and controllable genetic
205 “parts” with high dynamic range continue to hamper efforts in genome-scale mammalian
206 engineering²⁴⁻²⁶. Studies to reincorporate EAAs into the core mammalian metabolism could
207 provide greater understanding of nutrient-starvation in different physiological contexts including
208 the tumor microenvironment²⁷, help answer deep evolutionary questions regarding the formation
209 of the metazoan lineage²⁸, and lead to new model systems or even therapeutics to address
210 metabolic syndrome, Maple Syrup Urine Disease²⁹ and Phenylketonuria³⁰ all of which involve
211 amino acid biosynthetic dysfunction^{31,32}. Emerging synthetic genomic efforts to build a
212 prototrophic mammal may require reactivation of many more genes (**Table ED1-ED3**), iterations
213 of the design, build, test (DBT) cycle, and a larger coordinated research effort to ultimately bring
214 such a project to fruition.

215

216

217 **METHODS**

218

219 Pathway completeness analysis

220 For pathway completeness analysis, the EC numbers of each enzyme in each amino acid
221 biosynthesis pathway (excluding pathways annotated as only occurring in prokaryotes) were
222 collected from the MetaCyc database (**Table ED4**). Variant biosynthetic routes to the same
223 amino acid were considered as separate pathways, generating distinct EC number lists. The
224 resulting per-pathway EC number lists were checked against the KEGG, Entrez Gene, Entrez
225 Nucleotide, and Uniprot databases using their respective web APIs for each listed organism. If
226 the combination of all databases contained at least one complete EC numbers list,

227 corresponding to an end-to-end complete biosynthetic pathway, the organism was considered
228 “complete” for that essential amino acid.

229

230 Cell lines and media

231 CHO Flp-In™ cells (ThermoFisher, R75807) were used in all experiments. For growth assays
232 involving amino acid dropout formulations, medium was prepared from an amino acid-free
233 Ham’s F-12 (Kaighn’s) powder base (US Biological, N8545), and custom combinations of amino
234 acids were added back in as needed to match the standard amino acid concentrations for
235 Ham’s F-12 (Kaighn’s) medium or as specified. Custom amino acid dropout medium was
236 adjusted to a pH of 7.3, sterile filtered, and supplemented with 10% dialyzed Fetal Bovine
237 Serum and Penicillin-Streptomycin (100U/mL) prior to use. For metabolomics experiments,
238 medium was prepared from an amino acid-free and glucose-free RPMI 1640 powder base (US
239 Biological, R9010-01), and custom combinations of amino acids and isotopically heavy glucose
240 and sodium pyruvate were added in to match the standard amino acid concentrations for RPMI
241 1640 or as specified. pH was adjusted to 7.3, sterile filtered and supplemented with 10%
242 dialyzed Fetal Bovine Serum and Penicillin-Streptomycin (100U/mL) prior to use.

243

244 Cell counting and quantification

245 For amino acid dropout curves, cells were seeded at 1×10^4 into 6-well plates into F12-K media
246 with lowered amino acid concentrations relative to typical F12-K media and then allowed to
247 grow for five days. Media was then aspirated off and replaced with PBS with Hoechst 33342 live
248 nuclear stain for automated imaging and counting using a DAPI filter set on an Eclipse Ti2
249 automated inverted microscope. To count, an automated microscopy routine was used to image
250 5 random locations within each well at 10x magnification, and then the cells present in imaged
251 frames counted using automatic cell segregation and counting software. Given differences in
252 cell response to starvation, segregation and counting parameters were tuned each experiment,
253 but kept constant between starvation conditions and cells with and without the pathway. For
254 synthetic prototroph pathway tests, raw cell counts were performed using the Countess II
255 Automated Cell Counter (ThermoFisher, A27977) in accordance with the manufacturer’s
256 protocol, or using the Scepter 2.0 Handheld Automated Cell Counter (Milipore Sigma, C85360)
257 in accordance with the manufacturer’s protocol. Where indicated, relative cell quantification was
258 measured using PrestoBlue™ Cell Viability Reagent (ThermoFisher, A13261) in accordance
259 with the manufacturer’s protocol.

260

261 Culturing synthetic prototrophic cells without exogenous supply of valine

262 For long-term culture of synthetic prototrophic cells, cells were cultured in 50% conditioned
263 valine-free F12-K medium. Conditioned medium was generated by seeding 1×10^6 pMTIV cells
264 into 10mL complete F12-K medium on 10cm plates and replacing the medium with 10mL freshly
265 prepared valine-free F12-K medium the next day following a PBS wash step. Cells conditioned
266 the medium for 2 days at which point the medium was collected, centrifuged at 300xg for 3 mins
267 to remove potential cell debris, and collected in 150mL vats to reduce batch-to-batch variation.
268 This 100% conditioned medium was subsequently mixed in a 1:1 ratio with freshly prepared,
269 unconditioned valine-free medium to generate so-called 50% conditioned valine-free medium,
270 which was used throughout the long-term culturing process of synthetic prototrophic cells
271 without exogenous supply of valine, For long-term culturing, 1×10^5 pMTIV cells were seeded in
272 triplicate populations into complete medium in 6-well plates, (day -1) which was replaced with
273 50% conditioned valine-free medium the next day (day 0) following a PBS wash step. Cells
274 were counted at each passaging event and split at a 1:4, 1:2 or 3:4 proportion such that
275 approximately 2×10^6 cells were seeded at each passaging event as best possible.

276

277 DNA assembly, recovery and amplification

278 Integrated constructs were synthesized *de novo* in 3kb DNA segments with each segment
279 overlapping neighboring segments by 80. Assembly was conducted *in yeast* by co-
280 transformation of segments into *Saccharomyces cerevisiae*. After 2 days of selection at 30C on
281 Sc-URA, individual colonies were picked and cultured overnight. 1.5mL of each resulting yeast
282 culture was resuspended in 250ul of P1 resuspension buffer (Qiagen, 19051) containing RNase.
283 Glass beads were added to each resuspension and the mixture was vortexed for 10 mins to
284 mechanically shear the cells. Next, cells were subject to alkaline lysis by adding 250ul of P2
285 lysis buffer (Qiagen, 19052) for 5 mins and then neutralized by addition of Qiagen N3
286 neutralization buffer (Qiagen, 19053). Subsequently, cell debris was spun down and plasmid
287 DNA was collected using the Zymo Zyppy plasmid preparation kit (Zymo Research, D4036)
288 according to the manufacturer's instructions. Plasmid DNA was eluted in 30ul of Zyppy Elution
289 buffer of which 10ul would be transformed into 100ul of *E. coli* for plasmid amplification.

290

291 Protein extraction and western blot

292 Cell were lysed in SKL Triton lysis buffer (50 mM Hepes pH7.5, 150 mM NaCl, 1 mM EDTA, 1
293 mM EGTA, 10% glycerol, 1% Triton X-100, 25 mM NaF, 10 μ M $ZnCl_2$) supplemented with
294 protease inhibitor (Sigma 11873580001). NuPAGE™ LDS sample buffer (ThermoFisher,

295 NP0007) supplemented with 1.43 M β -mercaptoethanol was added to samples prior to heating
296 at 70°C for 10 mins. Gel electrophoresis was performed using 4-12% Bis-Tris gels
297 (ThermoFisher, NP0326BOX) and run in NuPAGE™ MOPS running buffer (ThermoFisher,
298 NP0001). Proteins were then transferred onto a PVDF membrane (Milipore Sigma, IPFL00010)
299 using the Biorad Trans-Blot Turbo system in accordance with the manufacturer's instructions.
300 The transfer membrane was blocked in Odyssey blocking buffer (LI-COR, 927-40000) for 1 h at
301 room temperature prior to incubation in primary antibody (Novus Biologicals, NBP2-59627
302 [1:1000 dilution]; Cell Signaling Technology, 2148 [1:1000 dilution]) solubilized in a 1:1 mixture
303 of Odyssey blocking buffer and TBS-T buffer (50 mM Tris Base, 154 mM NaCl, 0.1% Tween20)
304 overnight at 4°C. Secondary antibodies (LI-COR, 926-32210 [1:20,000 dilution]; LI-COR, 926-
305 68071 [1:20,000 dilution]), were also solubilized in Odyssey blocking buffer / TBS-T buffer. The
306 membrane was incubated in the secondary antibody solution for 1.5 h at room temperature.

307

308 Metabolomics

309 Cells were cultured in IH medium over 3 passages prior to cell harvest. Cell pellets were
310 generated by trypsinization, followed by low speed centrifugation, and the pellet was frozen at -
311 80°C until further processing. A metabolite extraction was carried out on each sample with an
312 extraction ratio of 1e6 cells per mL (80% methanol containing internal standards, 500 nM),
313 according to a previously described method³³. The LC column was a Millipore™ ZIC-pHILIC (2.1
314 x150 mm, 5 μ m) coupled to a Dionex Ultimate 3000™ system and the column oven temperature
315 was set to 25°C for the gradient elution. A flow rate of 100 μ L/min was used with the following
316 buffers; A) 10 mM ammonium carbonate in water, pH 9.0, and B) neat acetonitrile. The gradient
317 profile was as follows; 80-20%B (0-30 min), 20-80%B (30-31 min), 80-80%B (31-42 min).
318 Injection volume was set to 1 μ L for all analyses (42 min total run time per injection). MS
319 analyses were carried out by coupling the LC system to a Thermo Q Exactive HF™ mass
320 spectrometer operating in heated electrospray ionization mode (HESI). Method duration was 30
321 min with a polarity switching data-dependent Top 3 method for both positive and negative
322 modes, and targeted MS2 scans for the monoisotopic, U-13C, and U-13C/U-15N valine *m/z*
323 values. Spray voltage for both positive and negative modes was 3.5kV and capillary
324 temperature was set to 320°C with a sheath gas rate of 35, aux gas of 10, and max spray
325 current of 100 μ A. The full MS scan for both polarities utilized 120,000 resolution with an AGC
326 target of 3e6 and a maximum IT of 100 ms, and the scan range was from 67-1000 *m/z*. Tandem
327 MS spectra for both positive and negative mode used a resolution of 15,000, AGC target of 1e5,
328 maximum IT of 50 ms, isolation window of 0.4 *m/z*, isolation offset of 0.1 *m/z*, fixed first mass of

329 50 m/z, and 3-way multiplexed normalized collision energies (nCE) of 10, 35, 80. The minimum
330 AGC target was 1e4 with an intensity threshold of 2e5. All data were acquired in profile mode.
331 All valine data were processed using Thermo XCalibur Qualbrowser for manual inspection and
332 annotation of the resulting spectra and peak heights referring to authentic valine standards and
333 labeled internal standards as described.

334

335 RNA Seq

336 RNA was extracted from cells using the Qiagen RNeasy Kit (Qiagen, 74104) according to the
337 manufacturer's protocol. QIAshredder homogenizer columns were used to disrupt the cell
338 lysates (Qiagen, 79654). mRNA was purified using the NEBNext poly(A) mRNA Magnetic
339 Isolation module (New England Biolabs, E7490) in accordance with the manufacturer's protocol.
340 Libraries were prepared using the NEBNext Ultra RNA Library Prep Kit for Illumina (New
341 England Biolabs, E7770), and sequenced on a NextSeq 550 single-end 75 cycles high output
342 with v2.5 chemistry. Reads were adapter and quality trimmed with fastP using default
343 parameters and psuedoaligned to the GCF_003668045.1_CriGri-PICR Chinese hamster
344 genome assembly using kallisto. Differential gene enrichment analysis was performed with in R
345 with DESeq2 and GO enrichment performed and visualized with clusterProfiler against the
346 org.Mm.eg.db database, with further visualization with the pathview, GoSemSim, eulerr
347 packages.

348

349

350 **REFERENCES**

351

- 352 1 Payne, S. H. & Loomis, W. F. Retention and loss of amino acid biosynthetic pathways
353 based on analysis of whole-genome sequences. *Eukaryot Cell* **5**, 272-276,
354 doi:10.1128/EC.5.2.272-276.2006 (2006).
- 355 2 Akashi, H. & Gojobori, T. Metabolic efficiency and amino acid composition in the
356 proteomes of Escherichia coli and Bacillus subtilis. *Proc Natl Acad Sci U S A* **99**, 3695-
357 3700, doi:10.1073/pnas.062526999 (2002).
- 358 3 Seligmann, H. Cost-minimization of amino acid usage. *J Mol Evol* **56**, 151-161,
359 doi:10.1007/s00239-002-2388-z (2003).
- 360 4 Guedes, R. L. *et al.* Amino acids biosynthesis and nitrogen assimilation pathways: a great
361 genomic deletion during eukaryotes evolution. *BMC Genomics* **12 Suppl 4**, S2,
362 doi:10.1186/1471-2164-12-S4-S2 (2011).
- 363 5 Swire, J. Selection on synthesis cost affects interprotein amino acid usage in all three
364 domains of life. *J Mol Evol* **64**, 558-571, doi:10.1007/s00239-006-0206-8 (2007).

- 365 6 Zengler, K. & Zaramela, L. S. The social network of microorganisms - how auxotrophies
366 shape complex communities. *Nat Rev Microbiol* **16**, 383-390, doi:10.1038/s41579-018-
367 0004-5 (2018).
- 368 7 Wilson, A. C. & Duncan, R. P. Signatures of host/symbiont genome coevolution in insect
369 nutritional endosymbioses. *Proc Natl Acad Sci U S A* **112**, 10255-10261,
370 doi:10.1073/pnas.1423305112 (2015).
- 371 8 Isaacs, F. J. *et al.* Precise manipulation of chromosomes in vivo enables genome-wide
372 codon replacement. *Science* **333**, 348-353, doi:10.1126/science.1205822 (2011).
- 373 9 Mitchell, L. A. *et al.* Synthesis, debugging, and effects of synthetic chromosome
374 consolidation: synVI and beyond. *Science* **355**, doi:10.1126/science.aaf4831 (2017).
- 375 10 Fredens, J. *et al.* Total synthesis of *Escherichia coli* with a recoded genome. *Nature* **569**,
376 514-518, doi:10.1038/s41586-019-1192-5 (2019).
- 377 11 Boeke, J. D. *et al.* GENOME ENGINEERING. The Genome Project-Write. *Science* **353**, 126-
378 127, doi:10.1126/science.aaf6850 (2016).
- 379 12 Heng, B. C., Aubel, D. & Fussenegger, M. Prosthetic gene networks as an alternative to
380 standard pharmacotherapies for metabolic disorders. *Curr Opin Biotechnol* **35**, 37-45,
381 doi:10.1016/j.copbio.2015.01.010 (2015).
- 382 13 Tan, X., Letendre, J. H., Collins, J. J. & Wong, W. W. Synthetic biology in the clinic:
383 engineering vaccines, diagnostics, and therapeutics. *Cell* **184**, 881-898,
384 doi:10.1016/j.cell.2021.01.017 (2021).
- 385 14 Kitada, T., DiAndreth, B., Teague, B. & Weiss, R. Programming gene and engineered-cell
386 therapies with synthetic biology. *Science* **359**, doi:10.1126/science.aad1067 (2018).
- 387 15 Fischer, S., Handrick, R. & Otte, K. The art of CHO cell engineering: A comprehensive
388 retrospect and future perspectives. *Biotechnol Adv* **33**, 1878-1896,
389 doi:10.1016/j.biotechadv.2015.10.015 (2015).
- 390 16 Szymczak-Workman, A. L., Vignali, K. M. & Vignali, D. A. Design and construction of 2A
391 peptide-linked multicistronic vectors. *Cold Spring Harb Protoc* **2012**, 199-204,
392 doi:10.1101/pdb.ip067876 (2012).
- 393 17 O'Gorman, S., Fox, D. T. & Wahl, G. M. Recombinase-mediated gene activation and site-
394 specific integration in mammalian cells. *Science* **251**, 1351-1355,
395 doi:10.1126/science.1900642 (1991).
- 396 18 Hefzi, H. *et al.* A Consensus Genome-scale Reconstruction of Chinese Hamster Ovary Cell
397 Metabolism. *Cell Syst* **3**, 434-443 e438, doi:10.1016/j.cels.2016.10.020 (2016).
- 398 19 Cunningham, J. A., Liu, A. G., Bengtson, S. & Donoghue, P. C. The origin of animals: Can
399 molecular clocks and the fossil record be reconciled? *Bioessays* **39**, 1-12,
400 doi:10.1002/bies.201600120 (2017).
- 401 20 Amorim Franco, T. M. & Blanchard, J. S. Bacterial Branched-Chain Amino Acid
402 Biosynthesis: Structures, Mechanisms, and Drugability. *Biochemistry* **56**, 5849-5865,
403 doi:10.1021/acs.biochem.7b00849 (2017).
- 404 21 Zhenyukh, O. *et al.* High concentration of branched-chain amino acids promotes
405 oxidative stress, inflammation and migration of human peripheral blood mononuclear
406 cells via mTORC1 activation. *Free Radic Biol Med* **104**, 165-177,
407 doi:10.1016/j.freeradbiomed.2017.01.009 (2017).

- 408 22 Zhang, Y. *et al.* Expression of threonine-biosynthetic genes in mammalian cells and
409 transgenic mice. *Amino Acids* **46**, 2177-2188, doi:10.1007/s00726-014-1769-0 (2014).
- 410 23 Rees, W. D. & Hay, S. M. The biosynthesis of threonine by mammalian cells: expression
411 of a complete bacterial biosynthetic pathway in an animal cell. *Biochem J* **309 (Pt 3)**,
412 999-1007, doi:10.1042/bj3090999 (1995).
- 413 24 Black, J. B., Perez-Pinera, P. & Gersbach, C. A. Mammalian Synthetic Biology: Engineering
414 Biological Systems. *Annu Rev Biomed Eng* **19**, 249-277, doi:10.1146/annurev-bioeng-
415 071516-044649 (2017).
- 416 25 Gilbert, L. A. *et al.* Genome-Scale CRISPR-Mediated Control of Gene Repression and
417 Activation. *Cell* **159**, 647-661, doi:10.1016/j.cell.2014.09.029 (2014).
- 418 26 Weingarten-Gabbay, S. *et al.* Systematic interrogation of human promoters. *Genome*
419 *Res* **29**, 171-183, doi:10.1101/gr.236075.118 (2019).
- 420 27 Lim, A. R., Rathmell, W. K. & Rathmell, J. C. The tumor microenvironment as a metabolic
421 barrier to effector T cells and immunotherapy. *Elife* **9**, doi:10.7554/eLife.55185 (2020).
- 422 28 Tan, C. S. *et al.* Positive selection of tyrosine loss in metazoan evolution. *Science* **325**,
423 1686-1688, doi:10.1126/science.1174301 (2009).
- 424 29 Dancis, J., Levitz, M. & Westall, R. G. Maple syrup urine disease: branched-chain keto-
425 aciduria. *Pediatrics* **25**, 72-79 (1960).
- 426 30 Blau, N., van Spronsen, F. J. & Levy, H. L. Phenylketonuria. *Lancet* **376**, 1417-1427,
427 doi:10.1016/S0140-6736(10)60961-0 (2010).
- 428 31 Kemmer, C. *et al.* Self-sufficient control of urate homeostasis in mice by a synthetic
429 circuit. *Nat Biotechnol* **28**, 355-360, doi:10.1038/nbt.1617 (2010).
- 430 32 Ye, H. *et al.* Pharmaceutically controlled designer circuit for the treatment of the
431 metabolic syndrome. *Proc Natl Acad Sci U S A* **110**, 141-146,
432 doi:10.1073/pnas.1216801110 (2013).
- 433 33 Pacold, M. E. *et al.* A PHGDH inhibitor reveals coordination of serine synthesis and one-
434 carbon unit fate. *Nat Chem Biol* **12**, 452-458, doi:10.1038/nchembio.2070 (2016).
- 435

436 437 **Acknowledgements**

438 We would like to thank the members of the Boeke and Wang labs for comments and discussion
439 on the work and manuscript. RMM additionally thanks personal support from Xiaoyu Weng.

440 **Funding**

441 Defense Advanced Research Projects Agency HR0011-17-2-0041 (HHW, JDB)
442 National Institutes of Health / National Human Genome Research Institute RM1 HG009491 (JDB)
443 National Science Foundation MCB-1453219 (HHW)
444 Burroughs Wellcome Fund PATH1016691 (HHW)
445 Irma T. Hirschl Trust (HHW)
446 Dean's Fellowship from the Graduate School of Arts and Sciences of Columbia University (RMM)

447 **Author contributions**

448 RMM, JT, JDB and HHW developed the initial concept. JT, RMM, AK, SP, HB, SG, LL, MJS, XG,
449 DRJ, and AM performed experiments and analyzed the results. The overall project was
450 supervised by HHW and JDB. The manuscript was drafted by JT, RMM, JDB, and HHW with input
451 from all authors.

452 **Competing interests**

453 Jef D. Boeke is a Founder and Director of CDI Labs, Inc., a Founder of Neochromosome, Inc, a
454 Founder and SAB member of ReOpen Diagnostics, and serves or served on the Scientific
455 Advisory Board of the following: Sangamo, Inc., Modern Meadow, Inc., Sample6, Inc., Tessera
456 Therapeutics, Inc. and the Wyss Institute.

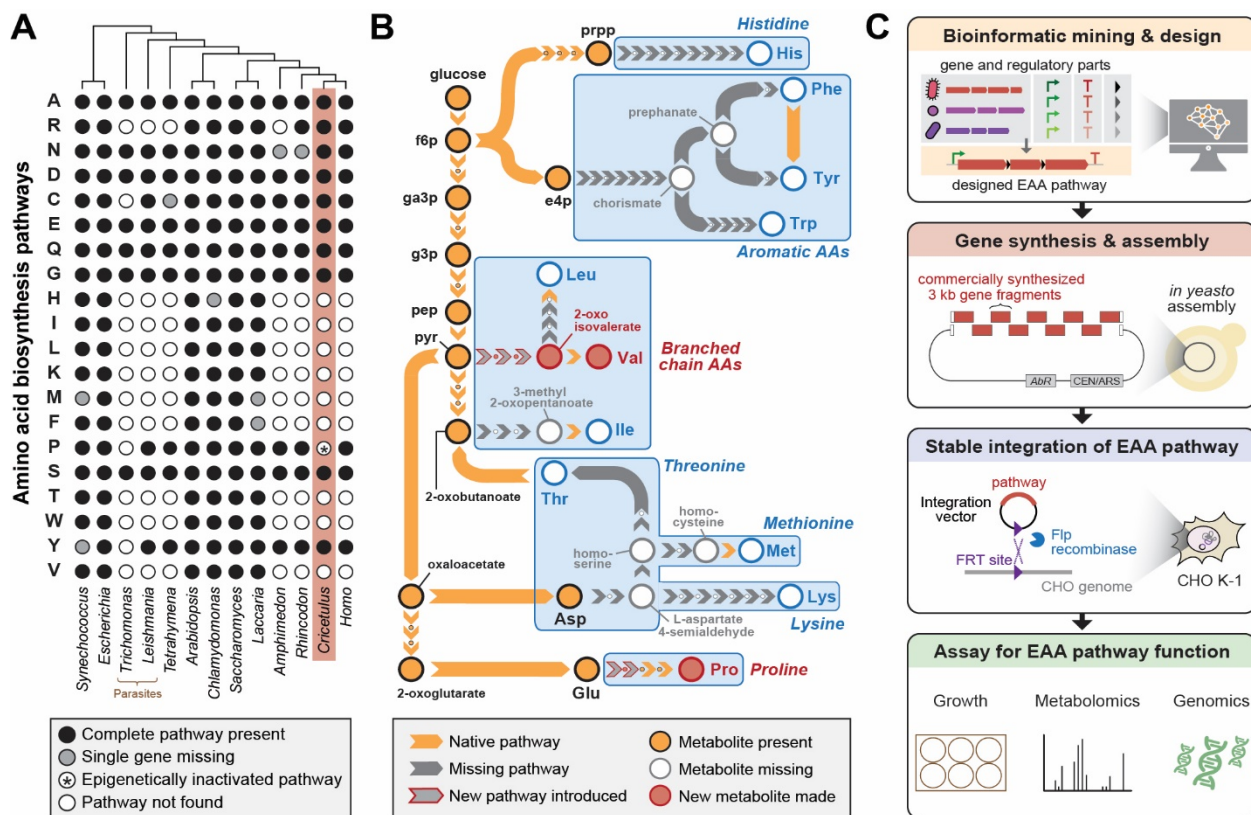
457 **Data and materials availability**

458 Sequencing data generated for this study is deposited in the NCBI SRA at accession number
459 PRJNA742028 (pending).

460

461 **FIGURES**

462



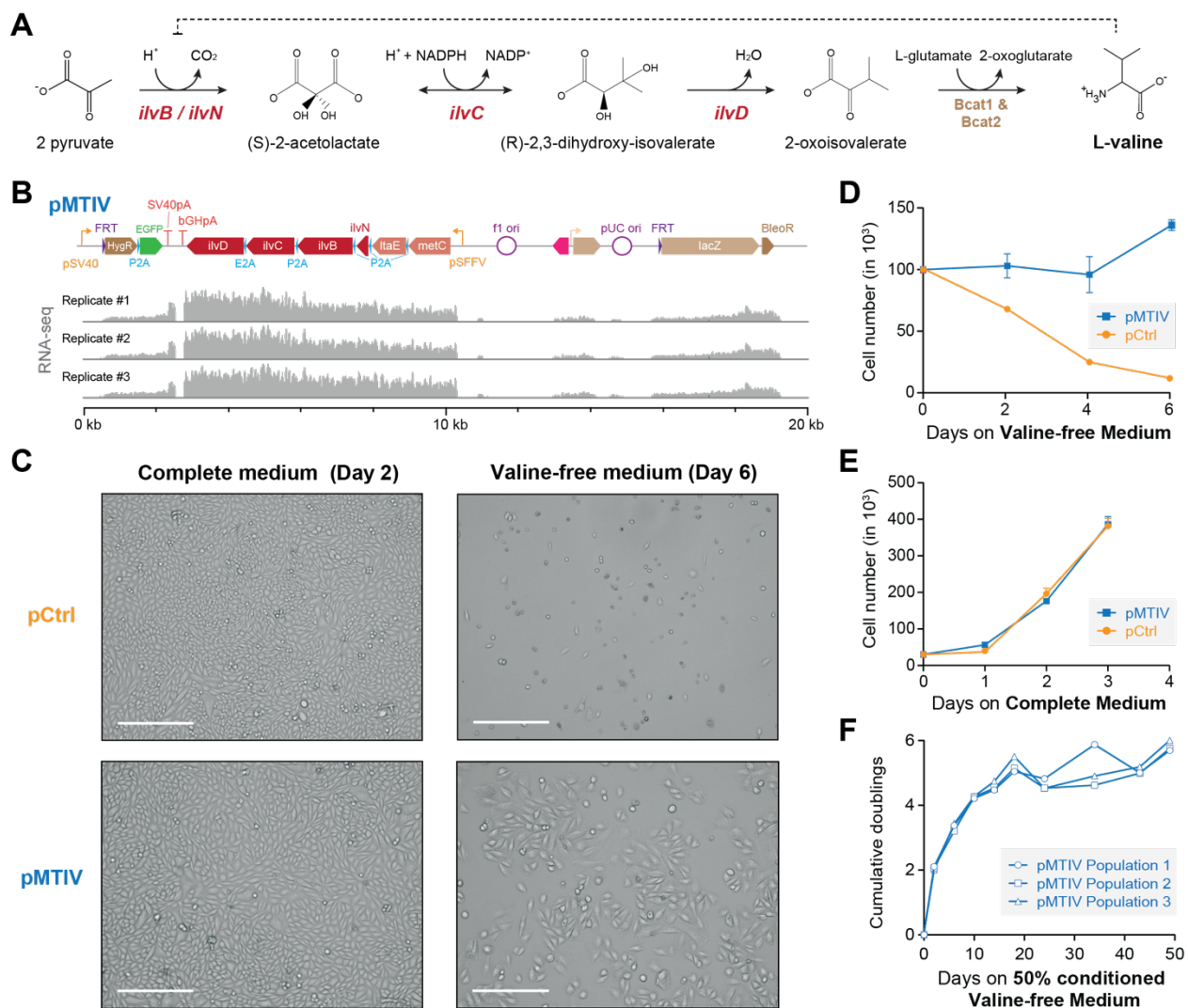
463

464

465 **Figure 1. Engineering Essential Amino Acid (EAA) biosynthesis in metazoan cells.**

466 **(A)** Presence of amino acid biosynthesis pathways across representative diverse organisms on
 467 Earth. **(B)** Schematic of EAA biosynthesis pathway steps that require engineering in mammalian
 468 cells to enable complete amino acid prototrophy if imported from *E. coli*. Proline and Valine
 469 pathways shown in this work are highlighted in red. **(C)** Workflow diagram of a synthetic genomics
 470 approach pathway design, construction, integration and testing towards mammalian EAA
 471 restoration.

472

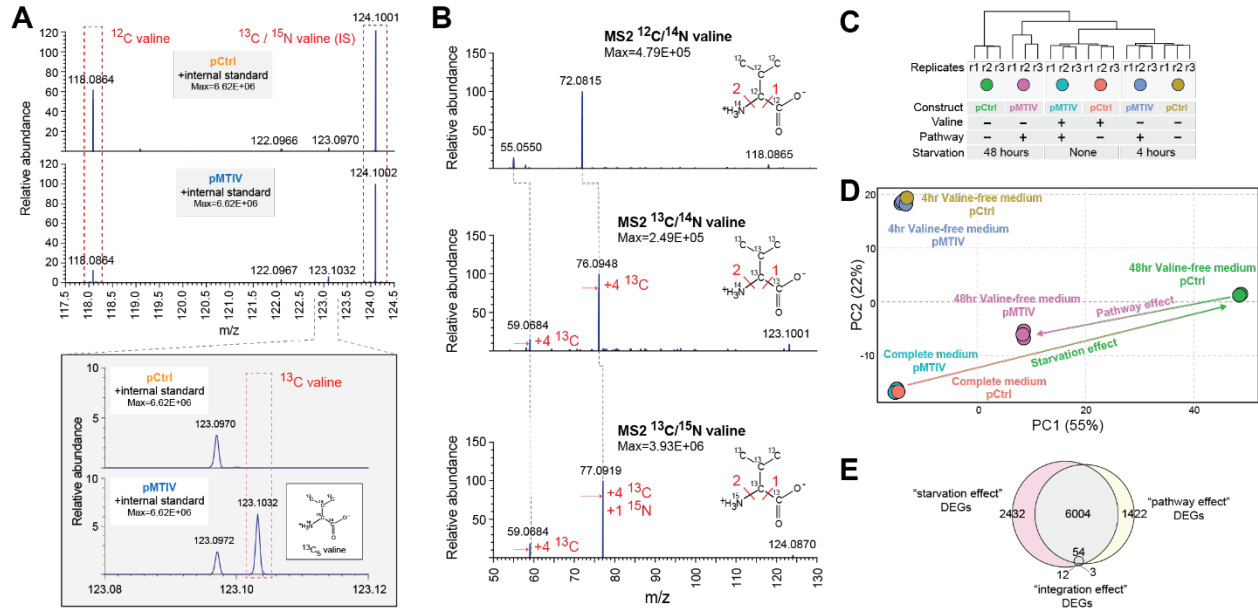


473
474

475 **Figure 2. Restoration of a Valine biosynthesis pathway in CHO-K1 cells.**

476 **(A)** Three enzymatic steps encoded by *E. coli* genes *ilvN*, *ilvB*, *ilvC*, and *ilvD* are required for
477 valine biosynthesis in CHO-K1 cells. **(B)** Schematic of pMTIV construct after genomic integration
478 and RNA-seq read coverage showing successful incorporation and active transcription. **(C)**
479 Microscopy images of CHO-K1 cells with integrated pCtrl or pMTIV constructs in Complete
480 Medium after 2 days or valine-free medium after 6 days. Scale bar = 300 μm. **(D)** Growth curve
481 of CHO-K1 cells with pCtrl or pMTIV in valine-free medium. Day 0 indicates number of seeded
482 cells. Triplicate population were plated for each timepoint in each of three 24-well wells, error bars
483 show the standard deviation or replicates. **(E)** Growth curve of CHO-K1 cells with pCtrl or pMTIV
484 in complete medium. Day 0 indicates number of seeded cells. Triplicate populations were plated
485 for each timepoint in each of three 24-well wells. Error bars show the standard deviation of

486 replicates **(F)** CHO-K1 with pMTIV cultured over 9 passages in 50% conditioned valine-free
487 medium.



488

489

490 **Figure 3. Heavy-carbon validation of endogenous valine production and transcriptomic**
 491 **signatures associated with rescue of nutritional starvation**

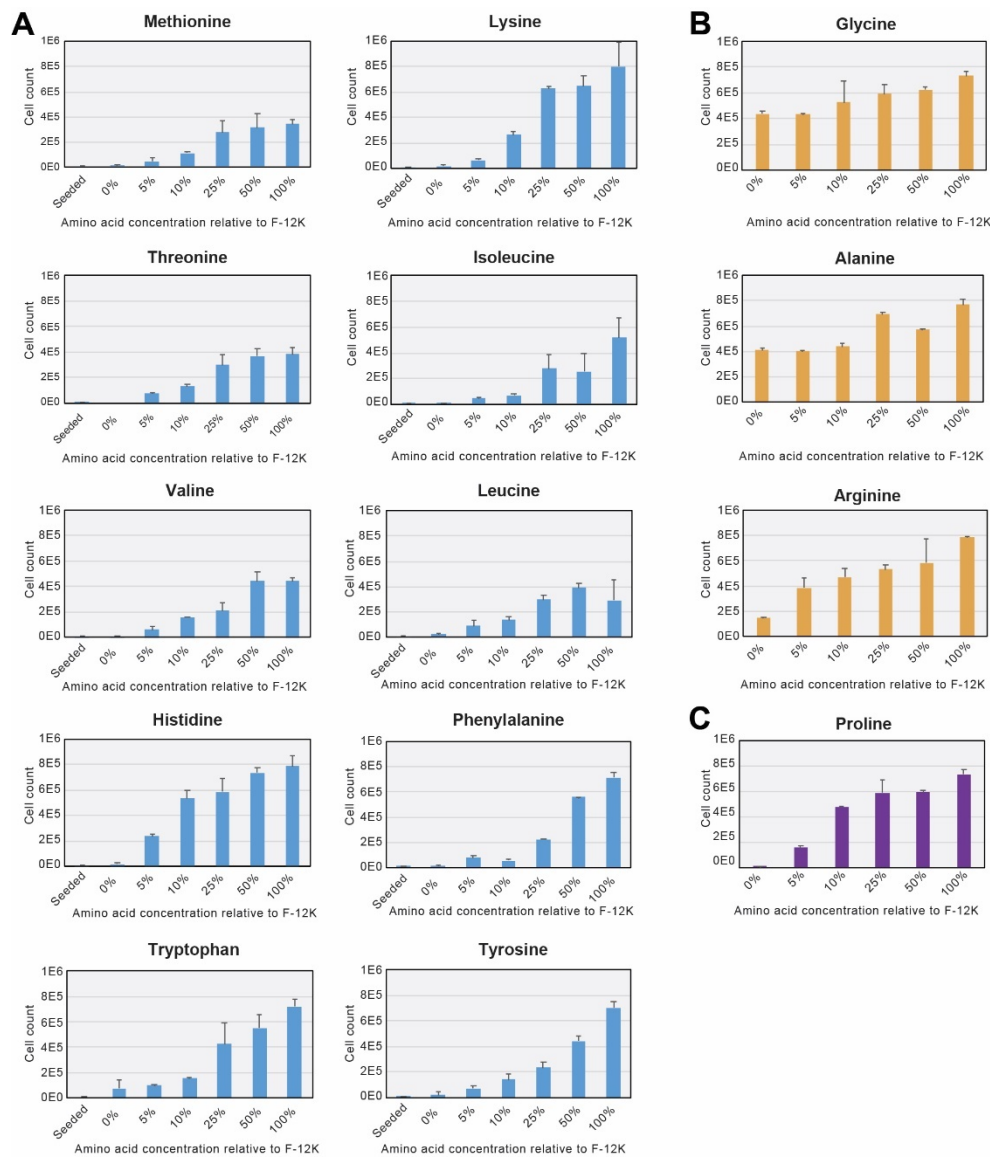
492 **(A)** Mass spectra showing an MS1 peak corresponding to the expected m/z for ^{13}C -valine when
 493 pMTIV cells were grown on valine-free medium supplemented with ^{13}C -glucose and ^{13}C -pyruvate,
 494 indicating autogenous production of intracellular valine. **(B)** MS2 performed on peaks extracted
 495 from pMTIV sample, which corresponded to m/z values expected for ^{12}C -valine, ^{13}C -valine and
 496 internal standard $^{13}\text{C}/^{15}\text{N}$ -valine. MS2 fragmentation patterns for each of these metabolites
 497 matched expectations. **(C)** RNAseq dendrogram of cells with and without the pMTIV pathway
 498 grown on complete medium or starved of valine for 4 or 48 hours. **(D)** PCA space depiction of
 499 cells with or without the pMTIV pathway grown on complete medium, or starved of valine for 4 or
 500 48 hours. **(E)** Overlap between Differently Expressed Genes (DEGs) comparing cells without the
 501 pathway cultured in valine-free medium to cells cultured in complete medium (the "starvation
 502 effect"), cells with and without the pMTIV pathway after 48 hours starvation on valine-free medium
 503 (the "pathway effect"), and cells with and without the pathway grown on complete medium (the
 504 "integration effect").

505

506

507 **EXTENDED DATA**

508

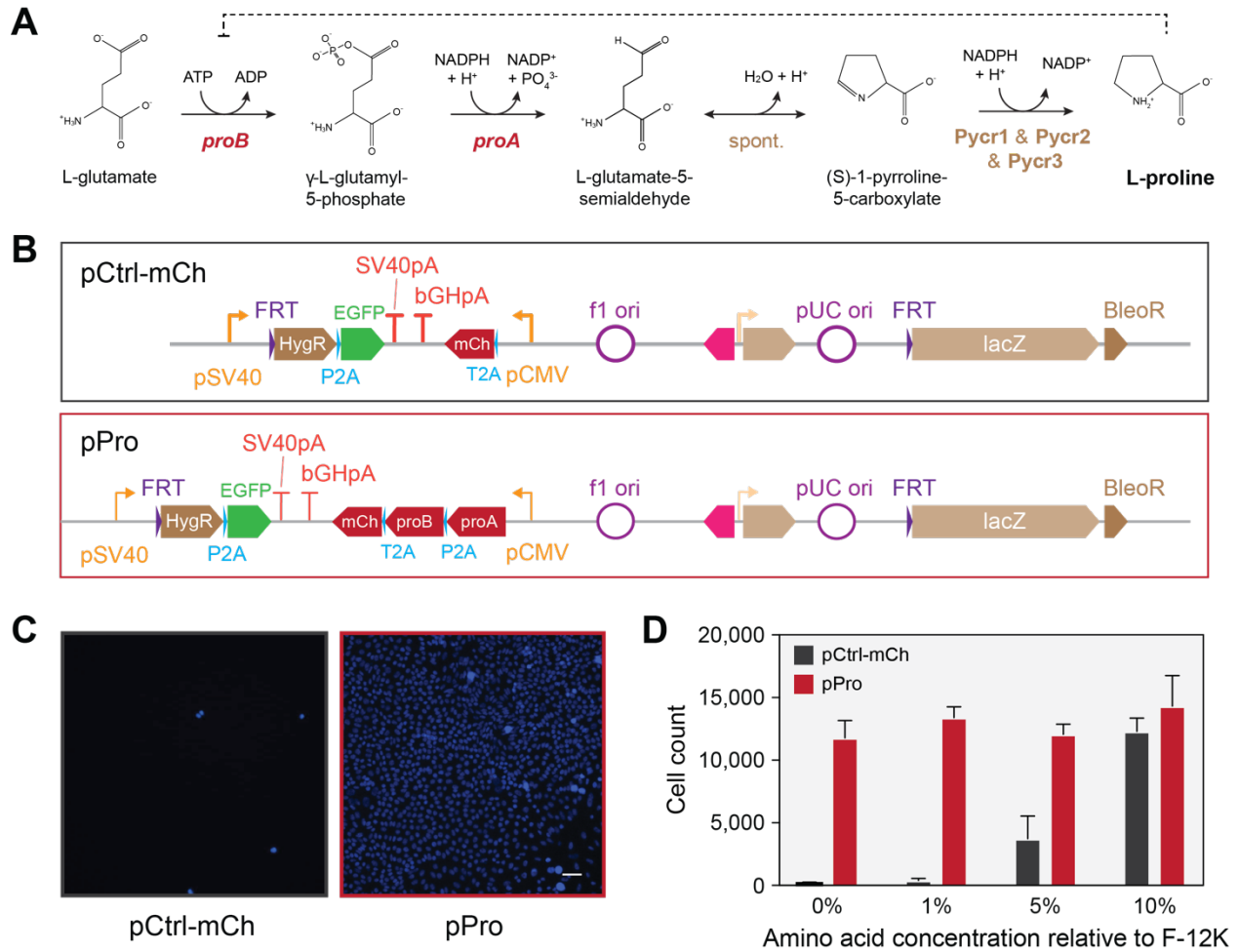


509

510 **Figure ED1. Amino acid dropout growth assays in CHO-K1.**

511 **(A)** Growth assays on CHO-K1 cells seeded into media with reduced or omitted essential amino
 512 acids. Percentages represent the relative media amino acid concentration compared to
 513 standard F-12K medium. 100% corresponds to 0.02 mM (Trp), 0.05 mM (Tyr), 0.06 mM (Ile,
 514 Met, Phe), 0.2 mM (Ala, Asn, Asp, Glu, Gly, Leu, Ser, Thr, Val), 0.22 mM (His), 0.4 mM (Cys,
 515 Lys), 0.6 mM (Pro), and 2 mM (Arg, Gln), respectively. Error bars show standard deviation of
 516 three replicates. **(B)** CHO-K1 cells grow with minimal defects in medium lacking glycine and
 517 alanine, but are more sensitive to arginine starvation. **(C)** CHO cells do not grow without

518 exogenous proline, confirming the known epigenetic proline auxotrophy found in this cell line.
519 Error bars show standard deviation of three replicates.
520



521

522 **Figure ED2. Imported bacterial genes rescue CHO epigenetic proline auxotrophy**

523 **(A)** Proline biosynthetic pathway from glutamate. **(B)** Schematic representation of two

524 constructs to test bacterial gene rescue of of CHO-K1 auxotrophy, one expressing the *E. coli*

525 *proA* and *proB* genes, and a control construct expressing only mCherry. Constructs are shown

526 as they appear following integration into the FLP-In CHO line. **(C)** Hoechst 33348 live nuclei

527 microscopy shows cells expressing the pPro construct grow in the absence of proline and

528 appear healthy. Scale bar indicates 50 μ m and is shared across images **(D)** Growth assay of

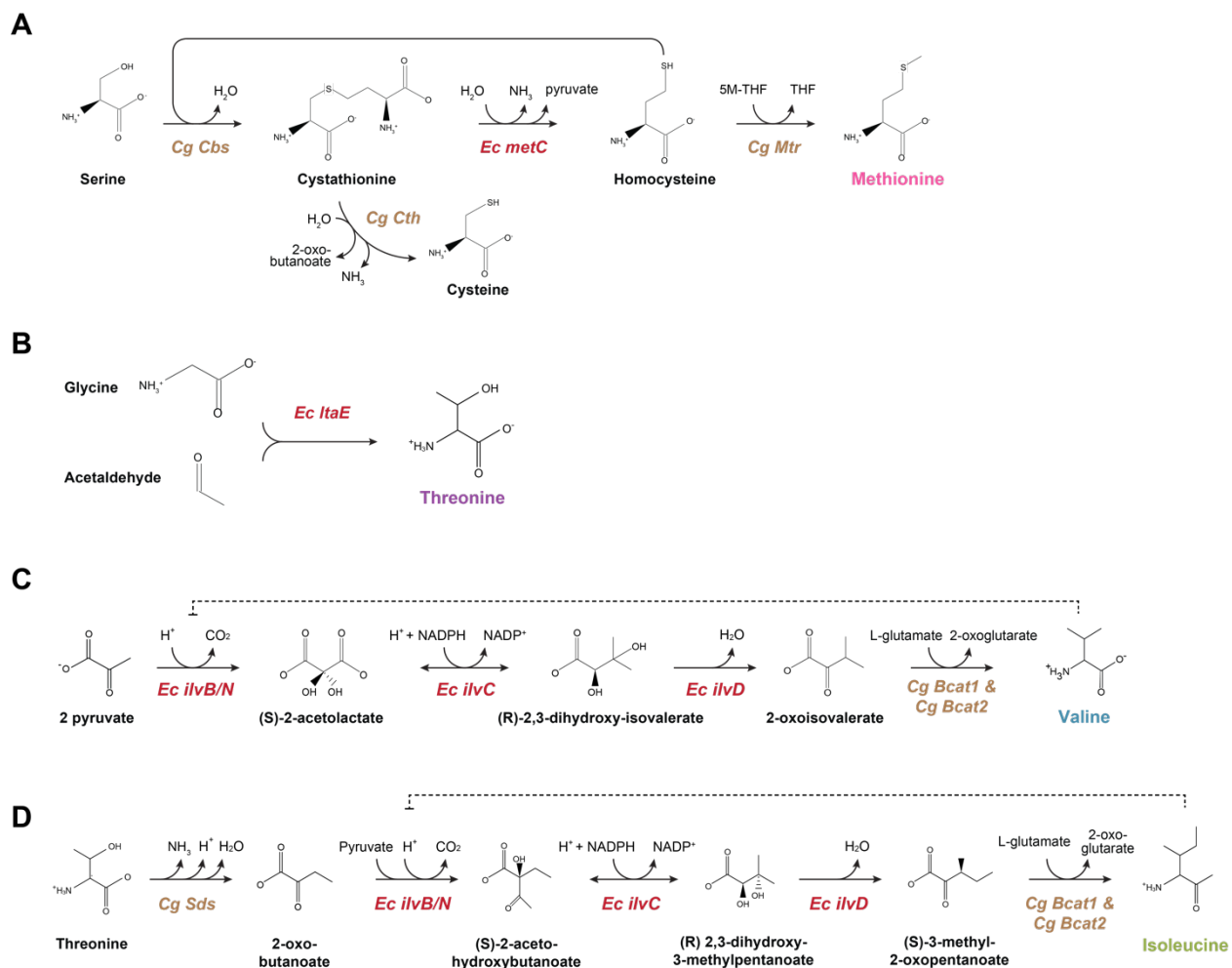
529 cells seeded into proline free medium and grown for 5 days. The bacterial gene pPro pathway

530 resulted in robust growth recovery in proline-free medium. Error bars show standard deviation of

531 three replicates.

532

533

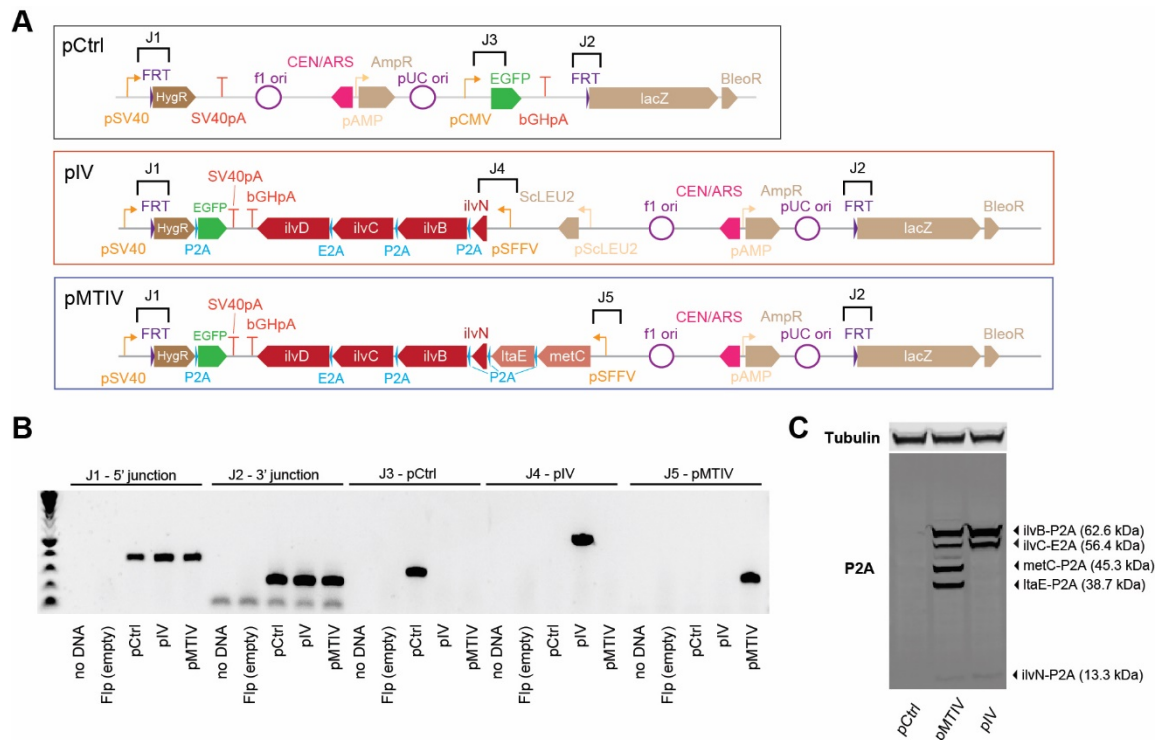


534

535 **Figure ED3. Schematic outlines of the MTIV pathways.**

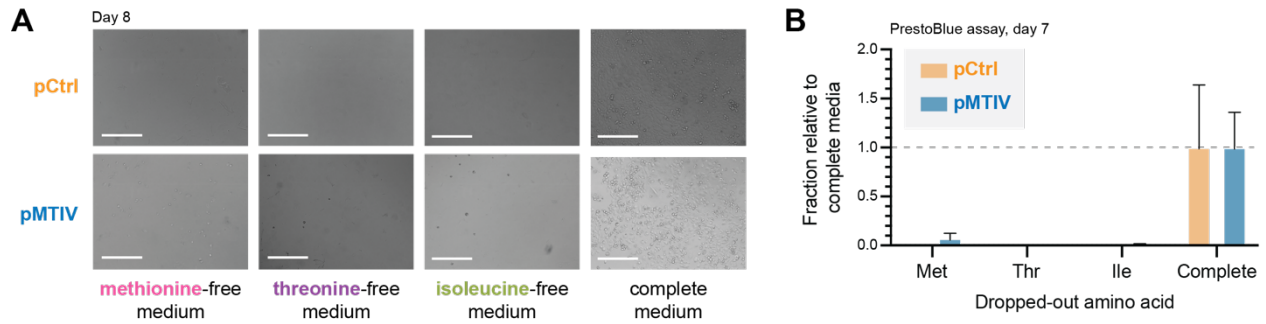
536 **(A)** Pathway for methionine biosynthesis. **(B)** Pathway for threonine biosynthesis. Note the
 537 shared multifunctional enzymes in **(C)** and **(D)** responsible for both isoleucine and valine
 538 production. In all panels “*Ec*” refers to *E. coli*, and “*Cg*” to *C. griseus*, the native CHO parental
 539 organism.

540



541
 542 **Figure ED4. Confirmation of BCAA biosynthetic construct integration and 2A peptide**
 543 **processing by PCR and Western blot**
 544 **(A)** Construct were designed with PCR landing pads flanking fragment junctions for rapid
 545 screening during construct assembly *in yeast*, shown above construct diagrams with brackets.
 546 **(B)** PCRs across these junctions confirm correct assembly of the control, pMTIV, and pIV
 547 constructs. **(C)** Immunoblotting against P2A peptides in pMTIV and pIV cells confirms 2A
 548 peptides are processed as expected. Note that *ilvD* (65.5 kDa) is not detectable because it lacks
 549 a terminal P2A tag.
 550

551

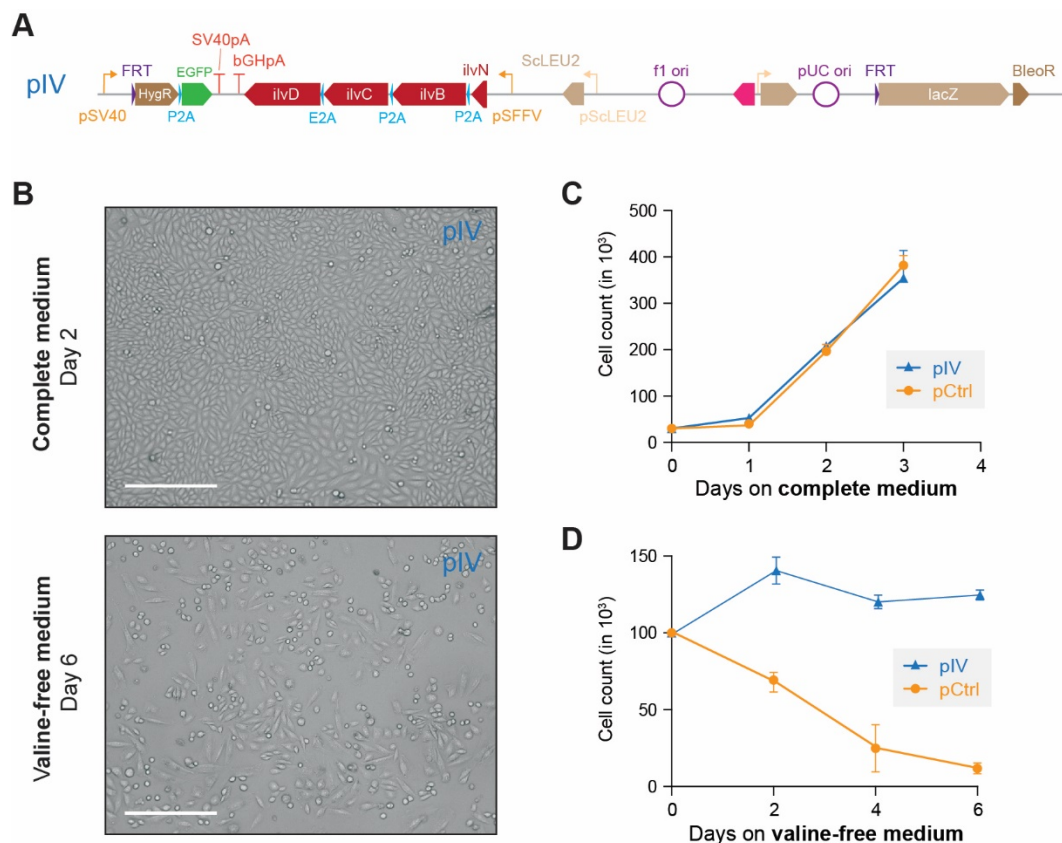


552

553 **Figure ED5. Lack of rescue of methionine, threonine and isoleucine auxotrophy by pMTIV**
554 **construct in CHO-K1 cells.**

555 **(A)** Phase-contrast images of cells carrying either pMTIV and pCtrl constructs after 8 days'
556 growth on EAA-free media (three leftmost panels) or complete medium (rightmost panel). Scale
557 bar represents 300um. **(B)** PrestoBlue™ cell viability assay of growth on EAA-free or complete
558 media after 7 days' growth. Error bars show standard deviation of three replicates.

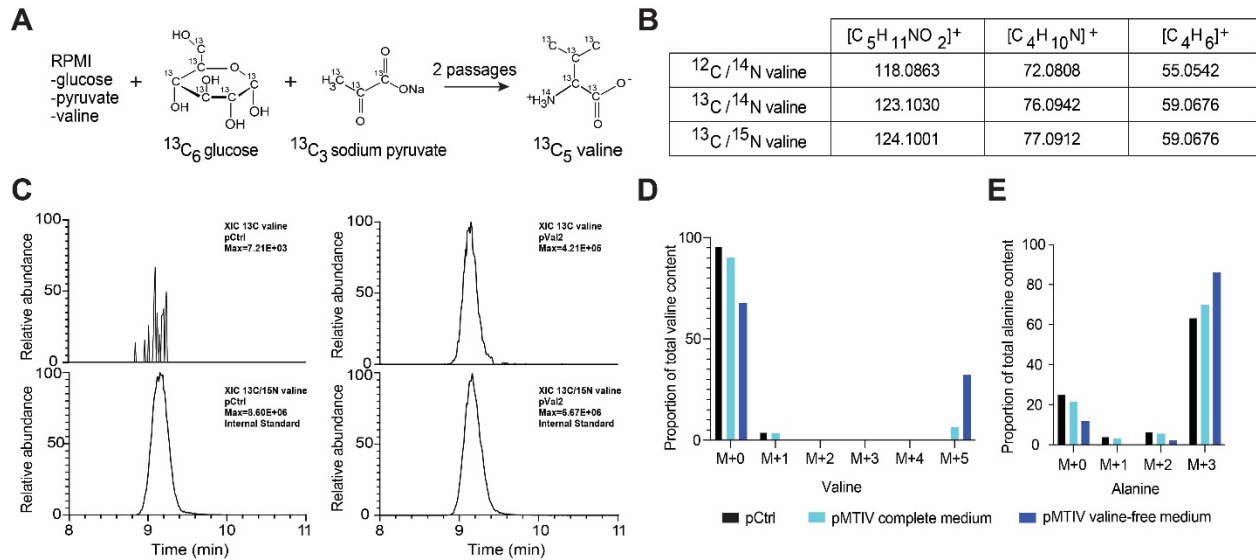
559



560
561
562
563
564
565
566
567
568
569

Figure ED6. The pIV construct rescues valine auxotrophy

(A) The minimized four-gene construct pIV lacking *ItaE* and *metC* after integration into the CHO genome. (B) Microscopy of pIV cells in both complete and valine-free medium. The pIV constructs rescue cellular morphology in valine-free medium. Scale bar = 300 μ m. (C) Growth of pIV construct in complete medium. Error bars show standard deviation of three replicates. (D) Live cell counting of pIV cells grown on conditioned valine-free medium. Error bars show standard deviation of three replicates.



570

571 **Figure ED7. Heavy-labeled metabolomics confirms endogenous valine production**

572 **(A)** Schematic outline of the ^{13}C labeling strategy for detection of biosynthesized valine. **(B)**

573 Expected m/z ratios for ^{12}C -valine, ^{13}C -valine, and spiked-in internal standard $^{13}\text{C}/^{15}\text{N}$ -valine in

574 unfragmented and fragmented states. **(C)** Extracted ion chromatography shows that the

575 presumed ^{13}C -valine found in pMTIV cells runs similarly to spiked-in internal standard $^{13}\text{C}/^{15}\text{N}$ -

576 valine, further confirming that ^{13}C -valine is produced in pMTIV cells. The presence of ^{13}C -valine

577 is specific to pMTIV cells and absent from control cells **(D)**. In theory, partial ^{13}C labeling of

578 valine is possible if just one of the two pyruvate substrates is ^{13}C -labelled. Partially ^{13}C -labeled

579 ($^{13}\text{C}_2$, $^{13}\text{C}_3$, $^{13}\text{C}_4$) valine species were below the level of detection. Therefore, the proportion of

580 $^{13}\text{C}_5$ -valine relative to total valine abundance within the cell can serve as a proxy for the degree

581 to which intracellular valine biosynthesis is meeting cellular valine demands. The lesser

582 occurrence of $^{13}\text{C}_1$ -valine can be explained by the natural abundance of ^{13}C . 32.2% of total

583 valine abundance in pMTIV cells cultured in valine-free medium was $^{13}\text{C}_5$ -labeled whereas the

584 corresponding proportion for pMTIV cells cultured in complete medium was 6.4% **(E)** Non-

585 essential amino acid alanine is biosynthesized from pyruvate and is not found in RPMI medium.

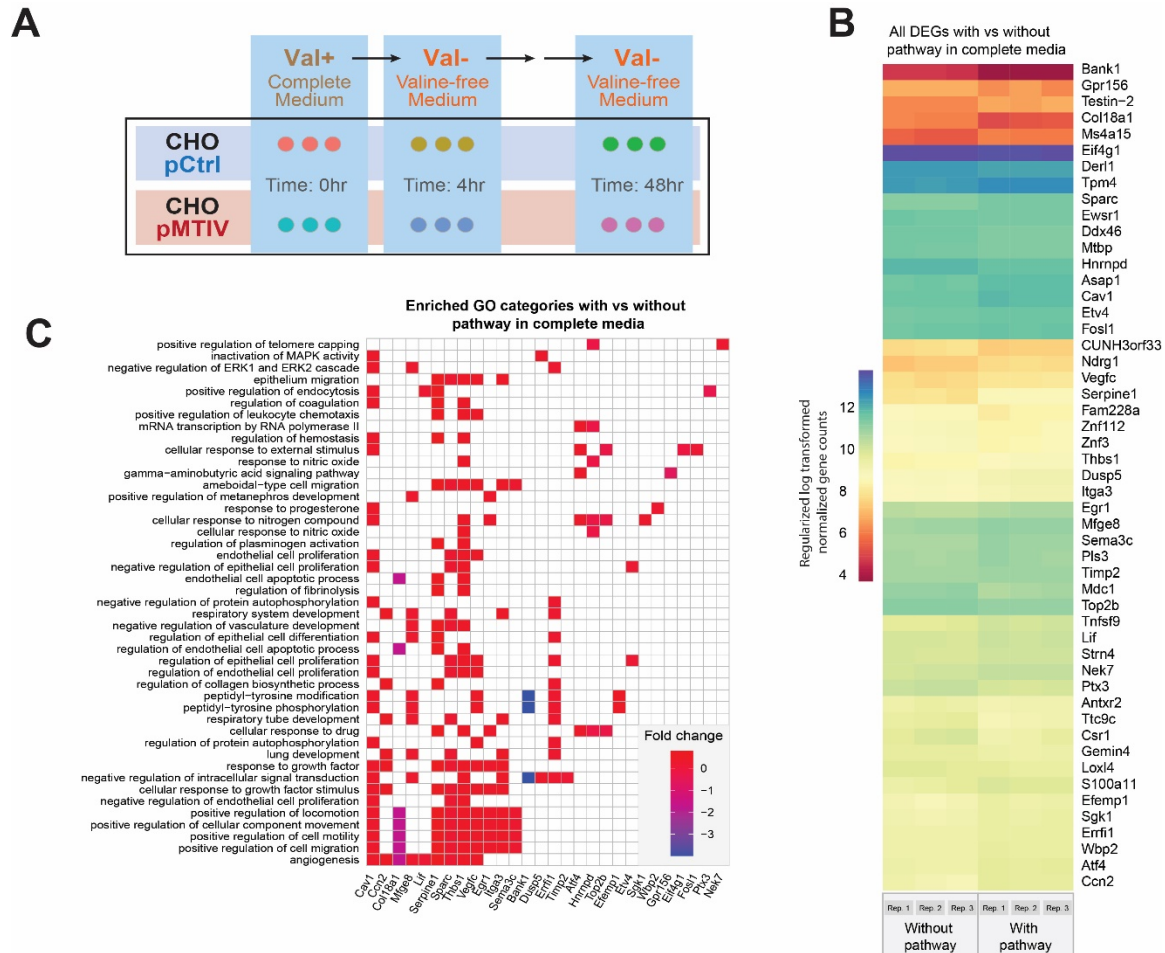
586 Alanine can thus serve a proxy for proteome turnover assuming similar usage rates for alanine

587 and valine. 86.1% of alanine was $^{13}\text{C}_3$ alanine in pMTIV cells cultured in valine-free RPMI

588 medium.

589

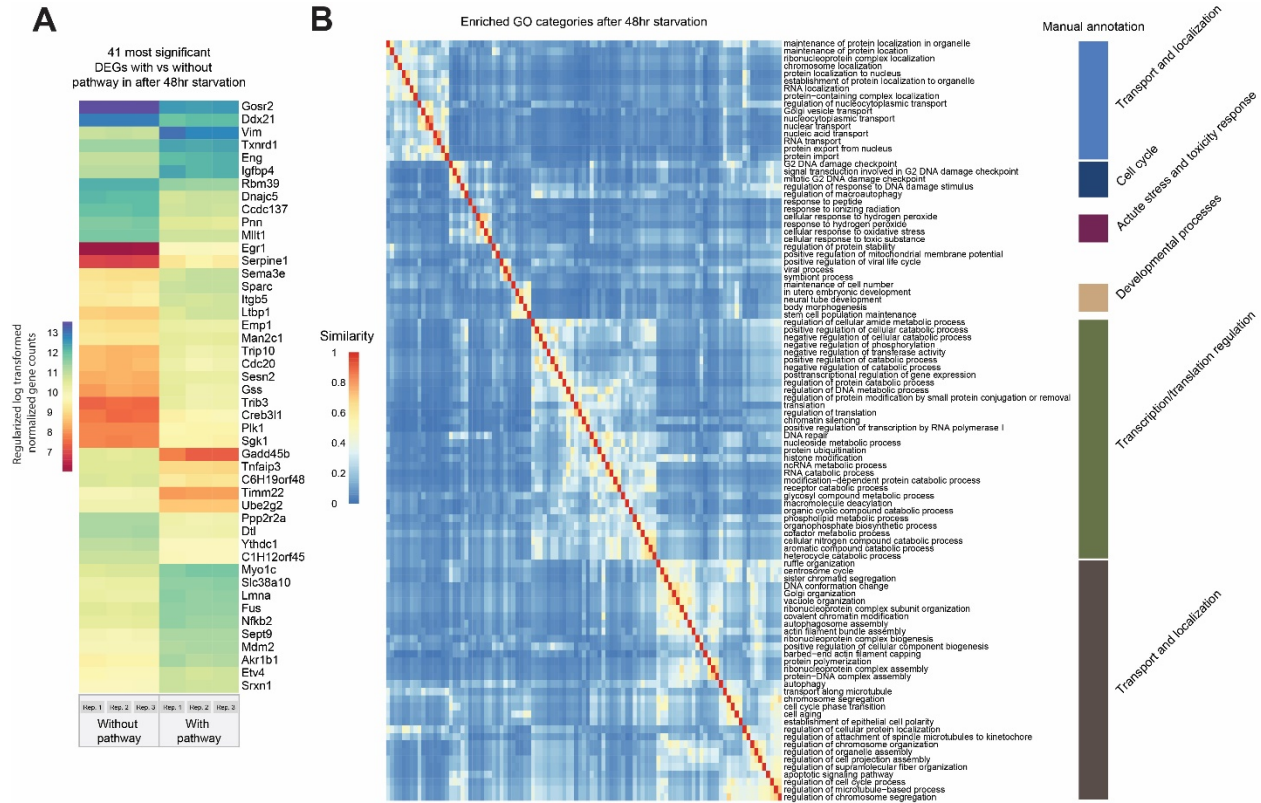
590



591
592
593
594
595
596
597
598
599

Figure ED8. Transcriptomic analysis of pMTIV pathway effect in Complete Medium.

(A) Schematic representation of the starvation regimen applied prior to collecting samples for transcriptomic analysis. (B) Regularized log fold changes in expression across the 51 differentially expressed genes when comparing cells with the pMTIV pathway to those without grown in complete medium. Values from three replicates are plotted side-by-side in each column. (C) GO category enrichment among the 51 differentially expressed genes.



600
601
602
603
604
605
606
607

Figure ED9. Transcriptional analysis of pMTIV pathway effect in Valine-free Medium.

(A) Regularized log transformed expression of the 50 most significant differentially expressed genes when comparing cells with the pMTIV pathway to those without after 48 hours of starvation in valine-free medium. Values from three replicates are plotted side-by-side in each column. **(B)** GO category enrichment among these genes, clustered and colored using a GO ontology distance metric, and manually grouped into larger supercategories, on the right.

Table ED1. Minimal prototrophic pathways set for AA prototrophy in mammalian cells

	Compound		EC reactions		Proposed genes	
AA: Histidine	Histidine (from PRPP)					
	2.4.2.17	Sc <i>HIS1</i>				
	3.6.1.31	Sc <i>HIS4</i>				
	3.5.4.19	Sc <i>HIS4</i>				
	5.3.1.16	Sc <i>HIS6</i>				
	4.3.2.10	Sc <i>HIS7</i>				
	4.2.1.19	Sc <i>HIS3</i>				
	2.6.1.9	Sc <i>HIS5</i>				
	3.1.3.15	Sc <i>HIS2</i>				
	1.1.1.23	Sc <i>HIS4</i>				
Enzymatic steps:	9					
Genes:			7			
Tryptophan	Chorismate (from E4P)		Tryptophan (from chorismate)			
	2.5.1.54	Sc <i>ARO3</i>	4.1.3.27	Sc <i>TRP2/3</i>		
	4.2.3.4	Sc <i>ARO1</i>	2.4.2.18	Sc <i>TRP4</i>		
	4.2.1.10	Sc <i>ARO1</i>	5.3.1.24	Sc <i>TRP1</i>		
	1.1.1.25	Sc <i>ARO1</i>	4.1.1.48	Sc <i>TRP3</i>		
	2.7.1.71	Sc <i>ARO1</i>	4.2.1.20	Sc <i>TRP5</i>		
	2.5.1.19	Sc <i>ARO1</i>				
	4.2.3.5	Sc <i>ARO2</i>				
	7		5			
		3		5		
Phenylalanine	Phenylalanine (from chorismate)					
	5.4.99.5	Ec <i>pheA</i>				
	4.2.1.51	Ec <i>pheA</i>				
	2.6.1.57	Ec <i>tyrB</i>				
	3					
		2				
Threonine	L-aspartate 4-semialdehyde (from aspartate)		Homoserine (from L-aspartate 4-semialdehyde)		Threonine (from homoserine)	
	2.7.2.4	Ec <i>metL</i>	1.1.1.3	Ec <i>metL</i> (redundant)	2.7.1.39	Ec <i>thrB</i>
	1.2.1.11	Ec <i>asd</i>			4.2.3.1	Ec <i>thrC</i>
	2		1		2	
		2		0		2
Methionine	Hydrogen sulfide (inorganic fixation)		Methionine (from hydrogen sulfide and homoserine)			
	2.7.7.4	Sc <i>MET3</i>	2.3.1.31	Sc <i>MET2</i>		
	2.7.1.25	Sc <i>MET14</i>	2.5.1.49	Sc <i>MET17</i>		
	1.8.4.8	Sc <i>MET16</i>	2.3.1.14	native		
	1.8.1.2	Sc <i>MET5/10</i>				
	4		3			
		5		2		
Lysine	Lysine (from L-aspartate 4-semialdehyde)					
	4.3.3.7	Cg <i>dapA</i>				
	1.17.1.8	Cg <i>dapB</i>				
	1.4.1.16	Cg <i>ddh</i>				
	4.1.1.20	Cg <i>lysA</i>				
	4					
		4				
Valine	2-oxoisovalerate (from pyruvate)		Valine (from 2-oxoisovalerate)			
	2.2.1.6	Ec <i>ilvB/N</i>	2.6.1.42	native		
	1.1.1.86	Ec <i>ilvC</i>				
	4.2.1.9	Ec <i>ilvD</i>				
	3		1			
		4		0		
Leucine	Leucine (from 2-oxoisovalerate)					
	2.3.3.13	Ec <i>leuA</i>				
	4.2.1.33	Ec <i>leuC/D</i>				
	1.1.1.85	Ec <i>leuB</i>				
	2.6.1.42	native				
	3					
		4				
Isoleucine	Isoleucine (from threonine)					
	4.3.1.19	native				
	2.2.1.6	Ec <i>ilvB/N</i> (redundant)				
	1.1.1.86	Ec <i>ilvC</i> (redundant)				
	4.2.1.9	Ec <i>ilvD</i> (redundant)				
	2.6.1.42	native				
	5		Total			
		0	32	Enzymatic steps		
			38	Genes		

Ec: *Escherichia coli*

Sc: *Saccharomyces cerevisiae*

Cg: *Corynebacterium glutamicum*

Table ED4. Complete amino acid prototrophy pathway EC numbers

Histidine 1						
2.7.6.1						
2.4.2.17						
3.6.1.31						
3.5.4.19						
5.3.1.18						
4.3.2.10						
4.2.1.19						
2.6.1.9						
3.1.1.15						
1.1.1.23						
Tryptophan (from E4P) 1						
2.5.1.54						
4.2.3.4						
4.2.1.10						
1.1.1.25						
2.7.1.71						
2.5.1.19						
4.2.3.5						
4.1.3.27						
2.4.1.18						
5.3.1.24						
4.1.1.48						
4.2.1.20						
Tyrosine (from E4P) 1.1	Tyrosine (from E4P) 1.2	Tyrosine (from E4P) 1.3	Tyrosine (from E4P) 1.4	Tyrosine (from E4P) 1.5	Tyrosine (from E4P) 1.6	Tyrosine (from Phe) 2
2.5.1.54	2.5.1.54	2.5.1.54	2.5.1.54	2.5.1.54	2.5.1.54	1.14.16.1
4.2.3.4	4.2.3.4	4.2.3.4	4.2.3.4	4.2.3.4	4.2.3.4	
4.2.1.10	4.2.1.10	4.2.1.10	4.2.1.10	4.2.1.10	4.2.1.10	
1.1.1.25	1.1.1.25	1.1.1.25	1.1.1.25	1.1.1.25	1.1.1.25	
2.7.1.71	2.7.1.71	2.7.1.71	2.7.1.71	2.7.1.71	2.7.1.71	
2.5.1.19	2.5.1.19	2.5.1.19	2.5.1.19	2.5.1.19	2.5.1.19	
4.2.3.5	4.2.3.5	4.2.3.5	4.2.3.5	4.2.3.5	4.2.3.5	
5.4.99.5	5.4.99.5	5.4.99.5	5.4.99.5	5.4.99.5	5.4.99.5	
1.3.1.13	1.3.1.13	1.3.1.13	1.3.1.13	2.6.1.79	2.6.1.79	
2.6.1.1	2.6.1.5	2.6.1.27	2.6.1.57		1.3.1.43	
Phenylalanine (from E4P) 1.1	Phenylalanine (from E4P) 1.2	Phenylalanine (from E4P) 1.3	Phenylalanine (from E4P) 1.4	Phenylalanine (from E4P) 1.5	Phenylalanine (from E4P) 1.6	
2.5.1.54	2.5.1.54	2.5.1.54	2.5.1.54	2.5.1.54	2.5.1.54	
4.2.3.4	4.2.3.4	4.2.3.4	4.2.3.4	4.2.3.4	4.2.3.4	
4.2.1.10	4.2.1.10	4.2.1.10	4.2.1.10	4.2.1.10	4.2.1.10	
1.1.1.25	1.1.1.25	1.1.1.25	1.1.1.25	1.1.1.25	1.1.1.25	
2.7.1.71	2.7.1.71	2.7.1.71	2.7.1.71	2.7.1.71	2.7.1.71	
2.5.1.19	2.5.1.19	2.5.1.19	2.5.1.19	2.5.1.19	2.5.1.19	
4.2.3.5	4.2.3.5	4.2.3.5	4.2.3.5	4.2.3.5	4.2.3.5	
5.4.99.5	5.4.99.5	5.4.99.5	5.4.99.5	5.4.99.5	5.4.99.5	
4.2.1.51	4.2.1.51	4.2.1.51	4.2.1.51	2.6.1.79	4.2.1.51	
2.6.1.1	2.6.1.5	2.6.1.27	2.6.1.57	4.2.1.91	2.6.1.57	
Serine (from G3P) 1.1	Serine (from G3P) 1.2	Serine (from G3P) 1.3	Serine (from Gly) 2			
1.1.1.95	3.1.3.38	3.1.3.38	2.1.2.1			
2.6.1.52	1.1.1.81	1.1.1.81				
3.1.3.3	2.6.1.45	2.6.1.51				
Methionine (from Asp) 1.1	Methionine (from Asp) 1.2	Methionine (from Asp) 1.3				
2.7.2.4	2.7.2.4	2.7.2.4				
1.2.1.11	1.2.1.11	1.2.1.11				
1.1.1.3	1.1.1.3	1.1.1.3				
2.7.1.39	2.3.1.31	2.3.1.31				
2.5.1.48	2.5.1.49	2.5.1.49				
4.4.1.13	2.3.1.13	2.3.1.14				
2.1.1.14						
Cysteine (from Ser) 1	Cysteine (from Met) 2.1	Cysteine (from Met) 2.2	Cysteine (from Asp) 3	Cysteine (from G3P) 4		
2.1.1.30	2.5.1.6	2.5.1.6	2.7.2.4	1.1.1.95		
2.5.1.47	2.1.1.37	2.1.1.37	1.2.1.11	2.6.1.52		
	3.3.1.1	3.2.2.9	1.1.1.3	2.5.1.65		
	4.2.1.22	3.3.1.1	2.3.1.31			
	4.4.1.1	4.2.1.22	2.5.1.49			
		4.4.1.1	4.2.1.22			
			4.4.1.1			
Threonine (from Asp) 1						
2.7.2.4						
1.2.1.11						
1.1.1.3						
2.7.1.39						
4.2.3.1						
Alanine (from pyr) 1	Alanine (from Cys) 2					
2.2.1.6	2.6.1.7					
1.1.1.86						
4.2.1.9						
2.6.1.42						
2.6.1.66						
Aspartate (from Glu) 1	Aspartate (from Asn) 2.1	Aspartate (from Asn) 2.2				
2.6.1.1	3.5.1.1	3.5.1.38				
Asparagine (from Asp) 1.1	Asparagine (from Asp) 1.2					
6.3.5.4	6.3.1.1					
Lysine (from 2-oxogl) 1.1	Lysine (from 2-oxogl) 1.2	Lysine (from 2-oxogl) 1.3	Lysine (from 2-oxogl) 1.4	Lysine (from Asp) 2		
2.3.3.14	2.3.3.14	2.3.3.14	2.3.3.14	2.7.2.4		
4.2.1.114	4.2.1.36	4.2.1.114	4.2.1.36	1.2.1.11		
1.1.1.87	1.1.1.87	1.1.1.286	1.1.1.286	4.3.3.7		
2.6.1.39	2.6.1.39	2.6.1.39	2.6.1.39	1.17.1.8		
1.2.1.95	1.2.1.95	1.2.1.95	1.2.1.95	2.6.1.83		
1.5.1.10	1.5.1.10	1.5.1.10	1.5.1.10	5.1.1.7		
1.5.1.7	1.5.1.7	1.5.1.7	1.5.1.7	4.1.1.20		
Glutamate (from Glu) 1	Glutamate (from 2-oxogl) 1.1	Glutamate (from 2-oxogl) 1.2	Glutamate (from 2-oxogl) 1.3	Glutamate (from 2-oxogl) 1.3		
1.4.1.13	1.4.1.3	1.4.1.4	1.4.1.14	1.4.7.1		
Glutamine (from Glu) 1						
6.3.1.2						
Arginine (from Glu) 1.1	Arginine (from Glu) 1.2	Arginine (from Glu) 1.3	Arginine (from Pro) 2			
2.3.1.1	2.3.1.1	2.7.2.11	1.5.5.2			
2.7.2.8	2.7.2.8	1.2.1.41	2.6.1.13			
1.2.1.38	1.2.1.38	2.6.1.13	6.3.5.5			
2.6.1.11	2.6.1.11	6.3.5.5	2.1.3.3			
3.5.1.16	2.1.3.35	2.1.3.3	6.3.4.5			
6.3.5.5	6.3.5.5	6.3.4.5	4.3.2.1			
2.1.3.3	2.1.3.3	4.3.2.1				
6.3.4.5	6.3.4.5					
4.3.2.1	4.3.2.1					
Proline (from Glu) 1	Proline (from Arg) 2.1	Proline (from Arg) 2.2	Proline (from Glu) 3.1	Proline (from Glu) 3.2	Proline (from Glu) 3.3	
2.7.2.11	3.5.3.6	3.5.3.6	2.7.2.11	2.7.2.11	2.7.2.11	
1.2.1.41	2.6.1.13	3.5.3.20	1.2.1.41	1.2.1.41	1.2.1.41	
1.5.1.2	2.6.1.13	2.6.1.13	2.6.1.13	2.6.1.13	2.6.1.13	
	1.5.1.2	1.5.1.2	2.6.1.13	2.6.1.8	2.6.1.8	
			1.5.1.2	1.5.1.1	1.5.1.1	
Glycine (from Ser) 1	Glycine (from Isoct) 2	Glycine (from Thr) 3.1	Glycine (from Thr) 3.2			
2.1.2.1	4.1.3.1	4.1.2.5	4.1.2.48			
	2.6.1.44					
Valine (from pyr) 1						
2.2.1.6						
1.1.1.86						
4.2.1.9						
2.6.1.42						
Leucine (from Val) 1.1	Leucine (from Val) 1.2					
2.3.1.13	2.3.1.13					
4.2.1.33	4.2.1.33					
1.1.1.85	1.1.1.85					
2.6.1.6	2.6.1.42					
Isoleucine (from Thr) 1						
4.3.1.19						
2.2.1.6						
1.1.1.86						
4.2.1.9						
2.6.1.42						